Chem

CellPress

Article

Electrolyzer Design for Flexible Decoupled Water Splitting and Organic Upgrading with Electron Reservoirs

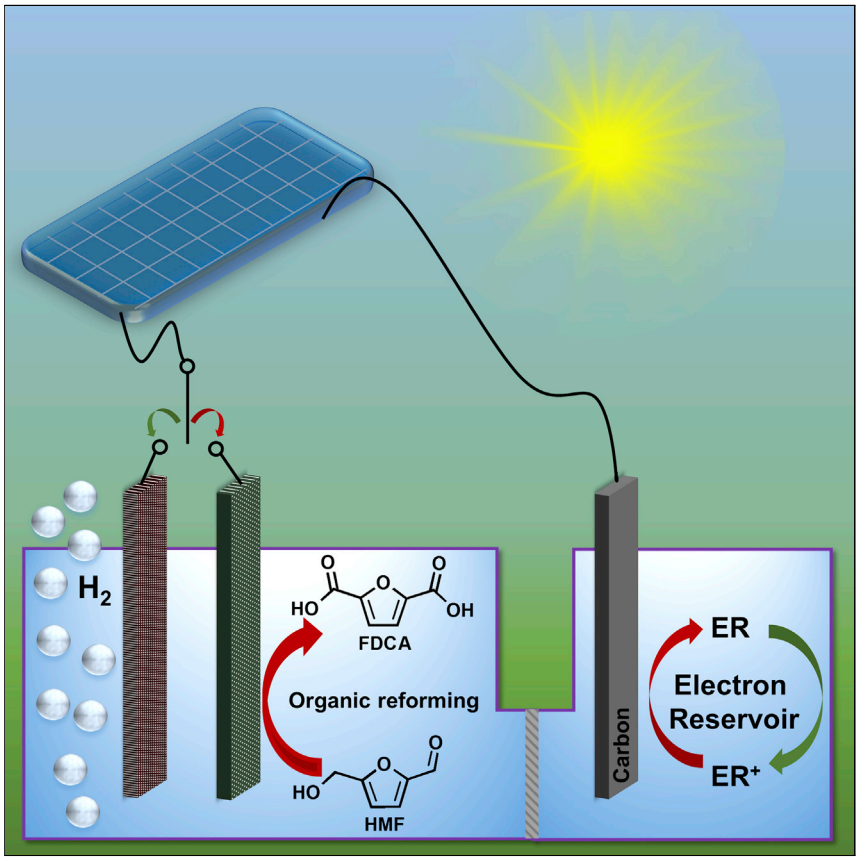

Robust proton-independent electron reservoirs of (ferrocenylmethyl) trimethylammonium chloride and $Na_4[Fe(CN)_6]$ are utilized to separate H_2 evolution from O_2 evolution with much lower voltage inputs than that of conventional water-splitting electrolysis. Such decoupled water splitting can be readily driven by photovoltaics with small photovoltages in near-neutral solution under natural sunlight irradiation. The electron reservoirs can facilitate sustainable H_2 production from decoupled water splitting and further integrate H_2 evolution with organic upgrading, yielding two value-added products (H_2 and 2,5-furandicarboxylic acid).

Wei Li, Nan Jiang, Bo Hu, ..., Tanner B. Hanson, T. Leo Liu, Yujie Sun

yujie.sun@usu.edu

HIGHLIGHTS

Stable proton-independent electron reservoirs of inexpensive iron complexes

Decoupling HER from OER in neutral electrolyte with small voltage inputs

Photovoltaic-driven decoupled water splitting under natural sunlight irradiation

Decoupled H_2 evolution integrated with valorization of biomass-derived intermediates

Li et al., Chem 4, 637–649
March 8, 2018
https://doi.org/10.1016/j.chempr.2017.12.019

Chem

CellPress

Article

Electrolyzer Design for Flexible Decoupled Water Splitting and Organic Upgrading with Electron Reservoirs

Wei Li,[1,2] Nan Jiang,[1,2] Bo Hu,[1] Xuan Liu,[1] Fuzhan Song,[1] Guanqun Han,[1] Taylor J. Jordan,[1] Tanner B. Hanson,[1] T. Leo Liu,[1] and Yujie Sun[1,3,*]

SUMMARY

Conventional water-splitting electrolysis drives the H_2 and O_2 evolution reactions (HER and OER, respectively) simultaneously with large voltage inputs. Herein, two inexpensive iron complexes as proton-independent electron reservoirs (ERs) are described for decoupled water electrolysis. (Ferrocenylmethyl) trimethylammonium chloride and $Na_4[Fe(CN)_6]$, which have proper redox potentials in aqueous media, are able to couple their oxidation with HER. The subsequent reduction of the oxidized ER^+ is then paired with OER. Both steps require much smaller voltage than that of direct water splitting. Nearly 100% Faradic efficiency and remarkable cycling stability were obtained for both ERs. Such decoupled water splitting could also be driven by photovoltaic cells with small photovoltages under sunlight irradiation. Furthermore, a two-step electrolysis of HER and the oxidation of 5-hydroxymethylfurfural mediated by $Na_4[Fe(CN)_6]$ was demonstrated under alkaline conditions, producing H_2 and 2,5-furandicarboxylic acid. This work presents a decoupled water electrolyzer design with great flexibility and safety advantages.

INTRODUCTION

H_2 production from water electrolysis with renewable energy inputs is a promising approach to the storage of renewable electricity in chemical forms.[1–4] Because of the thermodynamic requirements and slow kinetics of water splitting, conventional water electrolysis is usually conducted with a large voltage input (1.8–2.5 V) under either acidic or alkaline conditions with proton exchange membrane (PEM) electrolyzers or alkaline electrolyzers at elevated temperatures, respectively.[5,6] Regardless of the electrolyzer type, conventional water electrolysis always produces H_2 and O_2 simultaneously (Scheme 1A), and thus the rate of the H_2 evolution reaction (HER) is strictly dependent on the rate of the O_2 evolution reaction (OER).[7–9] Furthermore, the concurrence of HER and OER results in potential H_2/O_2 gas crossover, which is particularly severe at low current density (e.g., 10 mA cm^{-2}, a benchmark current density for solar-driven water splitting) and/or under high gas pressure, even if an ostensibly gas-impermeable membrane is utilized.[10–13] This will further require the downstream purification of H_2 (e.g., catalytic de-oxygenation). In addition, H_2/O_2 mixing may lead to the formation of reactive oxygen species because of the coexistence of H_2, O_2, and catalysts under electrocatalytic conditions, which would degrade the electrolyzer and shorten its operation lifetime.[14,15] Overall, these limitations of conventional water-splitting electrolysis call for an alternative electrolyzer design, not only circumventing these drawbacks but also enabling more flexibility in electrolyzer manufacture for a wide range of applications.

The Bigger Picture

Electrocatalytic water splitting is a green approach to producing clean H_2 fuel, especially when it is driven by renewable energy sources. Conventional water electrolysis always produces H_2 and O_2 simultaneously under corrosive acidic or alkaline conditions with large voltage inputs, posing safety concerns of H_2/O_2 mixing. Therefore, it is desirable to develop a new electrolyzer design for decoupled water splitting in an eco-friendly neutral solution with small voltage inputs to enable separated H_2 and O_2 evolution. Herein, we report (ferrocenylmethyl) trimethylammonium chloride and $Na_4[Fe(CN)_6]$ as proton-independent electron reservoirs for achieving separated H_2 and O_2 evolution in near-neutral solution driven by electricity or solar cells under sunlight irradiation. $Na_4[Fe(CN)_6]$ can also integrate H_2 evolution with organic oxidation to yield H_2 and high-value organic products. This work offers promising economic and safety advantages for sustainable H_2 production and organic transformation.

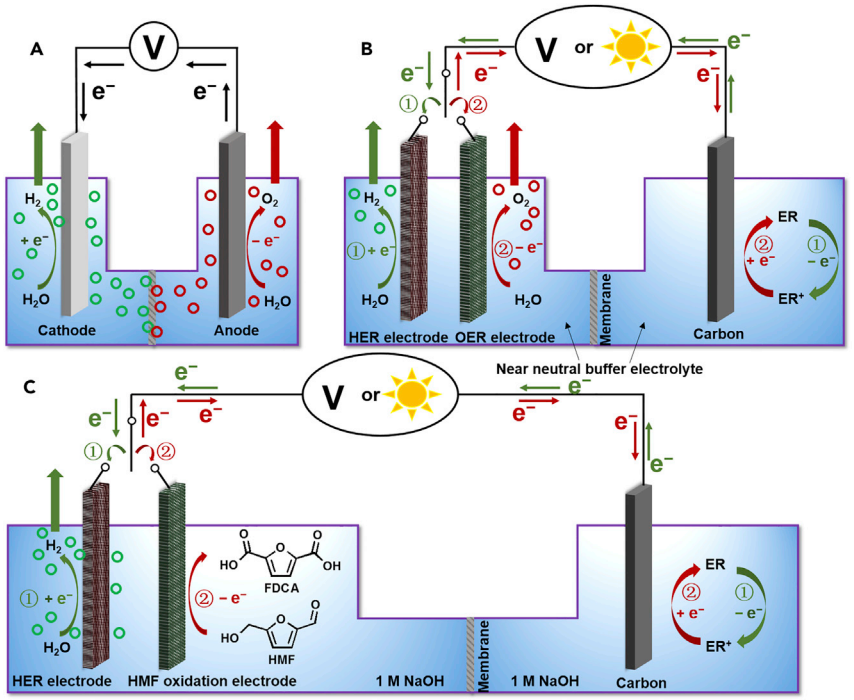

Scheme 1. Schematic Illustration of Electrolyzer Designs

(A) Conventional electrolyzer for one-step full water splitting.

(B) An electrolyzer design for decoupled water splitting with stepwise HER and OER in near-neutral electrolyte, wherein two working electrodes are alternatively utilized in the working compartment, and a carbon electrode is used in the counter compartment containing an electron reservoir of either FcNCl or $Na_4[Fe(CN)_6]$.

(C) An electrolyzer design for stepwise HER and organic oxidation in alkaline electrolyte (1 M NaOH). $Na_4[Fe(CN)_6]$ is introduced in the counter chamber with a carbon electrode.

For (B) and (C), ER and ER^+ denote the reduced (i.e., FcNCl or $[Fe(CN)_6]^{4-}$) and oxidized (i.e., $FcNCl^+$ or $[Fe(CN)_6]^{3-}$) forms of the adopted electron reservoir, respectively.

Recent years have witnessed the emergence of a decoupling strategy for water splitting, wherein redox mediators are used to decouple HER from OER. Representative proton-dependent redox mediators include phosphomolybdic acid and hydroquinone sulfonate.[8,12,16] The combination of V(III)/V(II) and Ce(IV)/Ce(III) redox mediators has also been used for indirect water electrolysis.[17,18] However, all of these redox mediators only function well in strongly acidic media, which are corrosive environments for the device and severely limit the scope of suitable electrocatalysts, particularly for OER,[19] as most of the earth-abundant transition-metal-based OER electrocatalysts cannot survive in strongly acidic electrolytes. The required proton migration between electrolyzer chambers also results in a great pH gradient and hence a large ohmic resistance.[20] Recently, a solid-state redox relay of $NiOOH/Ni(OH)_2$ was reported for alkaline water electrolysis, wherein HER and OER took place simultaneously in separate chambers with a fairly large voltage input (~2.1 V).[21] Nevertheless, $NiOOH/Ni(OH)_2$ is only stable under strongly alkaline conditions, and it requires a long pre-activation time before operation. Reversing current polarity or physically swapping two saturated $NiOOH/Ni(OH)_2$ electrodes is needed to regenerate the redox replays for electrolysis cycling.[21] Furthermore, the O_2 produced through the sluggish OER under alkaline conditions is not of significant value.[9,22] These limitations motivated us to develop alternative inexpensive electrolyzers of great convenience, flexibility, and durability for decoupled water

[1]Department of Chemistry and Biochemistry, Utah State University, Logan, UT 84322, USA

[2]These authors contributed equally

[3]Lead Contact

*Correspondence: yujie.sun@usu.edu

https://doi.org/10.1016/j.chempr.2017.12.019

electrolysis under benign conditions and preferably generating high-value products instead of O_2.

Herein, we demonstrate that a ferrocene-derived complex, (ferrocenylmethyl)trimethylammonium chloride (FcNCl), is able to act as a stable proton-independent electron reservoir to decouple HER from OER in near-neutral electrolyte (0.5 M Na_2SO_4). In addition, $Na_4[Fe(CN)_6]$ is used as a robust and low-cost proton-independent electron reservoir with a wider stable pH range from neutral to alkaline conditions not only for decoupled water splitting but also for H_2 production integrated with organic upgrading. By taking advantage of these two electron reservoirs, HER and OER, which have to take place simultaneously in one-step water splitting, are separated and coupled with the oxidation and reduction of electron reservoirs, respectively. Hence, HER and OER can occur at different times with different rates, and both steps require smaller voltage inputs than direct water splitting. The separation of HER from OER also eliminates the further downstream purification of H_2, reducing the cost and increasing the purity of H_2 fuel.[8] The neutral electrolyte enables us to utilize nonprecious-metal phosphide and Ni foam as electrocatalysts to catalyze HER and OER, respectively. Because of the substantially reduced voltage inputs for the decoupled water electrolysis, the H_2 and O_2 evolution can be driven by commercial photovoltaic (PV) cells with photovoltages (<1.7 V) lower than those of reported PV-driven water electrolysis. Thus, a wider solar spectrum could be utilized, expanding the candidate pool of semiconductors absorbing longer-wavelength sunlight for solar-driven water electrolysis without the need for many solar cells in series.[7,12,23] With the assistance of the alkaline stable $Na_4[Fe(CN)_6]$ electron reservoir, OER can be replaced with an organic oxidation to produce value-added product from a biomass-derived intermediate compound (e.g., 5-hydroxymethylfurfural). A two-step electrolysis of decoupled HER and organic oxidation is also successfully demonstrated. Overall, the use of proton-independent electron reservoirs enables great flexibility in electrolyzer design for decoupled water splitting, H_2 production, and organic upgrading. It allows the cathodic and anodic reactions in the working compartment to occur at different times, not only avoiding the H_2/O_2 mixing problem but also making both reaction rates independent of each other. The utilization of an environmentally benign neutral electrolyte further expands the pool of electrocatalyst candidates encompassing those inexpensive first-row transition-metal-based electrocatalysts and allows for potential integration with biocatalysts for the production of biofuels, bioproducts,[24–27] and seawater electrolysis.

RESULTS AND DISCUSSION

Principle for Decoupled Water Splitting and Integrated Organic Upgrading

The principle for decoupled water splitting in near-neutral solution is illustrated in Scheme 1B. An ideal electron reservoir should possess a reversible redox potential positioned between the electrocatalytic onset potentials of HER and OER in the same electrolyte. A two-compartment H cell is adopted with an ion exchange membrane. In the working chamber, both the HER (e.g., a transition-metal phosphide working electrode) and OER (e.g., a Ni foam working electrode) electrodes are placed, and a carbon counter electrode is positioned in the counter chamber containing the electron reservoir solution. In step 1, the HER working electrode is connected to the carbon counter electrode through an external power source. Upon an appropriate negative voltage bias applied to the HER working electrode, H_2 evolution takes place on it, and simultaneously oxidation of the electron reservoir occurs on the carbon counter electrode. In this case, the voltage input is smaller than

that required for full water splitting, given that the oxidation potential of the electron reservoir is less positive than the OER onset potential. After a certain amount of charge is passed (determined by the capacity of electron reservoir), step 2 switches the connection from the HER electrode to the OER electrode. When sufficient positive voltage bias is applied to the OER working electrode, O_2 evolution takes place, and meanwhile reduction of the oxidized electron reservoir (ER^+) back to its original state (ER) occurs on the carbon counter electrode. Such a positive voltage bias is also smaller than that for full water splitting, because the reduction potential of the oxidized electron reservoir is less negative than the HER onset potential. Under alkaline conditions, OER in step 2 can be replaced by electrochemical organic oxidation (Scheme 1C), such as the oxidation of 5-hydroxymethylfurfural (HMF) to 2,5-furandicarboxylic acid (FDCA), in that its required oxidation potential is less positive than that of OER. Under this scenario, a large voltage input for one-step water splitting is separated into two smaller voltage inputs for individual HER, OER, or organic upgrading, which can be readily driven by PV cells of small photovoltages. The key to the success of this decoupling strategy is to find a suitable electron reservoir complex.

Selection Criteria of Electron Reservoir

As alluded to in the above discussion, an ideal electron reservoir for decoupled water electrolysis should satisfy the following criteria: (1) high solubility in water, (2) fast and reversible proton-independent redox feature positioned between the HER and OER onset potentials, (3) strong robustness for repeated redox cycling, and (4) low-cost composition and synthesis from abundant materials. The (ferrocenylmethyl)trimethylammonium chloride, FcNCl, exhibits high water solubility and excellent electrochemical stability in a long cycling neural aqueous redox flow battery[28] and indeed meets all the criteria. FcNCl can be conveniently synthesized via direct alkylation of a commercially available precursor (ferrocenylmethyl)-dimethylamine (FcN) with methyl chloride in a yield of nearly unity.[28] Even though the precursor FcN is almost insoluble in water, the solubility of FcNCl dramatically increases to at least 4 M in water. The most critical feature of our electron reservoir, distinct from the reported proton-dependent redox mediators, is that the redox electrochemistry does not involve protonation or deprotonation for the proton-independent electron reservoir, eliminating the dependence on the use of strongly acidic electrolytes.[8,12,16] Instead, a mild near-neutral electrolyte (0.5 M Na_2SO_4) was used.

The electrochemistry of FcNCl was investigated via cyclic voltammetry and compared with the HER and OER onset potentials. As plotted in Figure 1, the cyclic voltammogram of 50 mM FcNCl in 0.5 M Na_2SO_4 (pH $\sim$ 6.5) showed a reversible redox couple at 0.40 V versus Ag/AgCl (saturated KCl) on a glassy carbon electrode. In the absence of electrocatalysts, HER and OER currents do not take off until -1.2 and 1.7 V versus Ag/AgCl, respectively, on carbon electrodes in 0.5 M Na_2SO_4. In near-neutral electrolyte, a large group of earth-abundant electrocatalysts can be used to reduce the voltage inputs for HER and OER.[29–36] Therefore, when a Ni foam decorated with Ni_2P (Ni_2P/Ni/NF) and a bare Ni foam (NF) were used as the HER and OER electrodes (Figures S1 and S2), respectively, the overpotentials for the two half reactions of water splitting were dramatically reduced (Figure 1). Nevertheless, the HER and OER still needed applied potentials beyond -1.0 and +1.0 V versus Ag/AgCl, respectively, to achieve appreciable catalytic current densities. Therefore, even with the assistance of water-splitting electrocatalysts, the redox potential of FcNCl was still well positioned between the HER and OER onsets. In addition, the scan-rate dependence of the cyclic voltammograms of FcNCl was also studied (Figure S3). The linear trend obtained from the variation of its

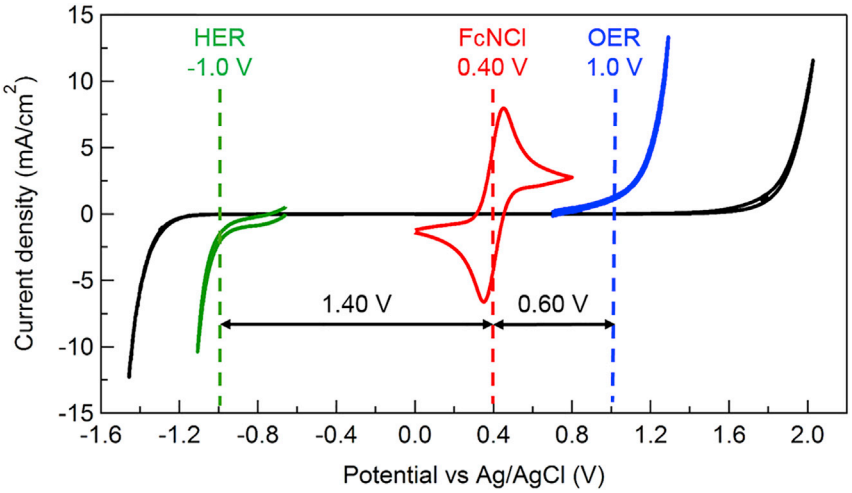

Figure 1. Comparison of the Cyclic Voltammograms of FcNCl, HER, and OER under Near-Neutral Conditions

All cyclic voltammetry curves were collected in a three-electrode configuration in 0.5 M Na_2SO_4 (pH 6.5) with Ag/AgCl (sat. KCl) as the reference electrode. Cyclic voltammogram of 50 mM FcNCl (red) was collected at a scan rate of 100 mV s^{-1} with a glassy carbon working electrode and carbon counter electrode. Cyclic voltammograms of HER (black) and OER (black) were collected on bare glassy carbon electrodes at a scan rate of 5 mV s^{-1} (iR corrected). Cyclic voltammograms (iR corrected) of HER on Ni_2P/Ni/NF (green) and OER on Ni foam (blue) were collected at a scan rate of 5 mV s^{-1} with a carbon counter electrode.

anodic and cathodic peak currents along the square root of the scan rate indicated that this redox process involved a molecular species in solution under diffusion control. The diffusion constant of FcNCl was further probed via a linear sweep voltammogram (LSV) using a rotating disk electrode (Figure S4). Calculations based on the derived Levich pot resulted in a diffusion constant of 0.71×10^{-6} cm^2 s^{-1} and an electron-transfer rate constant of 1.33×10^{-5} cm s^{-1} for FcNCl in 0.5 M Na_2SO_4, both of which were in good agreement with reported values for FcNCl and analogous complexes in aqueous media.[28]

Decoupled Water Electrolysis Using FcNCl

According to the aforementioned experimental results obtained in three-electrode configuration, we were confident that FcNCl could act as an electron reservoir for decoupled water electrolysis. As an initial attempt to evaluate the feasibility of our strategy, we utilized a two-electrode compartment H cell with an anion exchange membrane to collect the LSV of HER on Ni_2P/Ni/NF in 0.5 M Na_2SO_4. A carbon rod was utilized as the counter electrode. A negative voltage bias was applied to Ni_2P/Ni/NF, and no catalytic HER current was observed until scanning beyond −2.4 V (Figure 2A). However, upon the addition of 50 mM FcNCl in the counter electrode compartment, the catalytic HER current on Ni_2P/Ni/NF rose rapidly after −1.4 V, saving nearly 1 V voltage input in comparison with the above condition (step 1 in Scheme 1B). With an external bias of −1.8 V continuously applied to the Ni_2P/Ni/NF working electrode, the amount of H_2 produced in an air-tight H cell was quantified by gas chromatography (GC) and compared with the theoretically calculated amount, under the assumption that all the passed charge was utilized to form H_2. Figure 2B plots the GC-measured and theoretically calculated amounts of H_2, and the near overlap of these two H_2 evolution traces rendered a Faradic efficiency close to 100% for H_2 evolution. Note that only H_2 was produced during this electrolysis, and the corresponding anodic reaction was the oxidation of FcNCl to

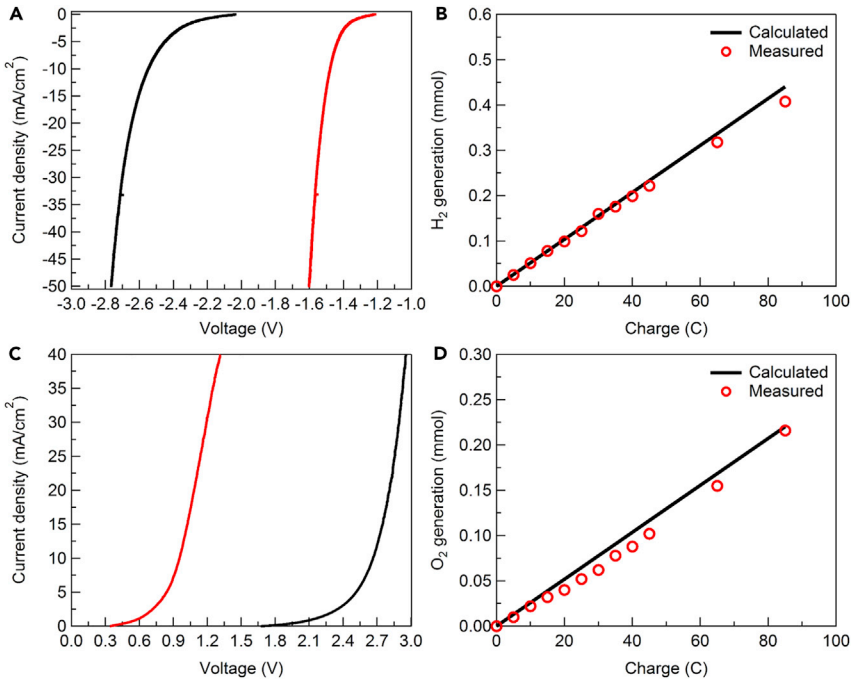

Figure 2. Electrochemical Investigation of Decoupled HER and OER with the Assistance of FcNCl as an Electron Reservoir

(A) Linear sweep voltammograms of Ni_2P/Ni/NF as the working electrode and a carbon rod as the counter electrode with 0 (black) or 50 mM (red) FcNCl and 0.5 M Na_2SO_4 in the counter chamber and only 0.5 M Na_2SO_4 in the working compartment (scan rate = 5 mV s^{-1}, iR corrected).

(B) Comparison of the GC-measured and theoretically calculated amounts of H_2 during electrolysis at −1.8 V under the same conditions as in (A) with FcNCl.

(C) Linear sweep voltammograms of NF as the working electrode and a carbon rod as the counter electrode with 0 (black) or 50 mM (red) $FcNCl^+$ and 0.5 M Na_2SO_4 in the counter chamber and only 0.5 M Na_2SO_4 in the working compartment (scan rate = 5 mV s^{-1}, iR corrected).

(D) Comparison of the GC-measured and theoretically calculated amounts of H_2 during electrolysis at 1.7 V under the same conditions as in (C) with $FcNCl^+$.

$FcNCl^+$ on the carbon counter electrode. No O_2 was detected in the headspace of the working chamber (Figure S5), indicating the high purity of H_2 product.

After the 50 mM FcNCl in the counter compartment had been fully oxidized, we switched the working electrode connection from the Ni_2P/Ni/NF electrode to the NF electrode (step 2 in Scheme 1B). Subsequently, a positive voltage bias was applied to NF to drive O_2 evolution. As displayed in Figure 2C, the catalytic OER current took off at merely 0.6 V. This is because the redox potential of $FcNCl^{+/0}$ (0.4 V versus Ag/AgCl) was relatively closer to the OER onset (~1.0 V versus Ag/AgCl) on NF (Figure 1). Nevertheless, in the absence of $FcNCl^+$ in the counter compartment, a much larger voltage input (>2.4 V) was required for conducting OER with the same electrodes. The GC-measured amount of O_2 also matched the theoretically calculated value very well (Figure 2D), confirming a Faradic efficiency of near unity for this decoupled O_2 evolution electrolysis at an applied bias of 1.7 V. In the meantime, no H_2 was detected in the working chamber (Figure S5). In fact, the cathodic reaction occurring in the counter compartment was the reduction of $FcNCl^+$ back to the FcNCl, thus accomplishing its regeneration cycle as an electron reservoir.

The voltage between Ni_2P/Ni/NF and carbon counter electrodes was −1.478 V to drive a current density of −10 mA cm^{-2} for HER in the presence of 50 mM FcNCl

(Figure 2A). In the second step for OER and $FcNCl^+$ reduction, a small voltage of 0.954 V was required for achieving the current density of 10 mA cm^{-2} (Figure 2C). If a Ni_2P/Ni/NF || NF electrode couple was used for one-step water splitting without any electron reservoir, a much larger voltage input of 2.338 V was required for producing 10 mA cm^{-2} in 0.5 M Na_2SO_4 (Figure S6). This demonstrates a high efficiency of 96% for two-step decoupled water splitting in relation to one-step direct water splitting. This efficiency is higher than that of the reported phosphomolybdic-acid-mediated (79%) and potassium hydroquinone-sulfonate-mediated (80%) decoupled water electrolyzers and comparable with that (93%) of a silicotungstic-acid-mediated system in acidic solution and a $Ni(OH)_2$-mediated decoupled water electrolysis system (92%) without considering resistive factors.[8,9,16,37] The practical energy efficiency of our decoupled water electrolyzer could be calculated by dividing the thermoneutral potential (i.e., 1.48 V, see details in Supplemental Information) of water electrolysis by the total applied voltage at room temperature,[38,39] when the Faradic efficiencies of HER and OER are both 100%. The calculated energy efficiency was 61% at 10 mA cm^{-2}, which is comparable with that of the silicotungstic-acid-mediated (63%), the potassium-hydroquinone-sulfonate-mediated (61%), or the phosphomolybdic-acid-mediated (59%) decoupled water electrolyzers, the Pt-based PEM electrolyzer (67%) in acidic electrolyte and the efficiency of a $Ni(OH)_2$-mediated Ir || Pt electrolyzer (67%) in 1 M NaOH solution at room temperature (Table S1).[8,16,21,37] When proton buffers were added in the electrolyte, we were able to collect the HER and OER LSVs at pH 5, 7, and 9 (Figures S7–S9). Within the pH range from 5 to 9, our FcNCl functioned well as an electron reservoir for decoupled water splitting.

In order to evaluate the robustness of FcNCl as an electron reservoir for repeated HER and OER electrolysis, we conducted long-term decoupled water electrolysis by alternating the applied voltage bias to the Ni_2P/Ni/NF and NF electrodes in 0.5 M Na_2SO_4, and the counter compartment was charged with a carbon electrode immersed in 10 mM FcNCl and 0.5 M Na_2SO_4. By alternating the applied voltage bias of −1.6 V to Ni_2P/Ni/NF for H_2 evolution and 1.8 V to NF for O_2 production, we carried out the decoupled water electrolysis such that each half cycle passed ~7 C charge before we switched the applied bias. Figure 3 displays the accumulated charge versus time for 20 successive cycles. At the beginning of each cycle, the pH of the electrolyte was 6.5. Upon completion of the HER step, the pH value in the working compartment increased to 9, which decreased back to 6.5 once the OER step was finished. The similarity of these 20 charge-versus-time cycles indicates the robust cycling performance of FcNCl for repeated oxidation and reduction. Apparently, the generation of H_2 and O_2 periodically in the working compartment did not affect the reversible redox chemistry of FcNCl in the counter compartment. We also used NO_3^- as a counter ion to replace Cl^- in FcNCl. The change of counter ion did not affect the redox feature of FcN^- (Figure S10). The performance of $FcN(NO_3)$ as an electron reservoir for decoupled water electrolysis was comparable with that of FcNCl in Figure S11.

Solar-Driven H_2 Production Decoupled from OER Using FcNCl

Light-driven H_2 evolution from water splitting has been widely recognized as a promising approach to storing renewable solar energy in green chemical forms (i.e., H_2).[7,21,23] By virtue of the remarkably reduced voltage input for decoupled water electrolysis using FcNCl as described above, it is feasible to conduct H_2 generation in near-neutral solution under natural sunlight irradiation if a single photovoltaic (PV) module with small photovoltage is used as the external power source. On the basis of the aforementioned results, we reasoned that the

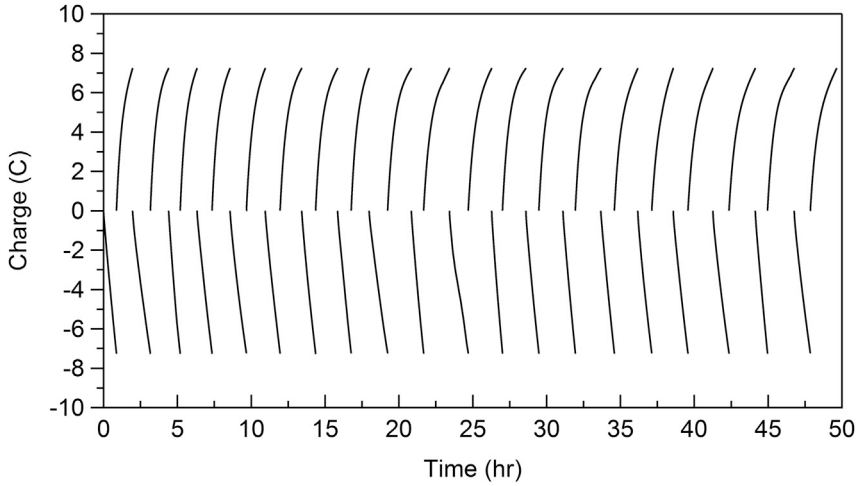

Figure 3. Electrolysis Cycles of HER and OER for Assessing the Stability of FcNCl as an Electron Reservoir

Charge evolution plot for repeated two-electrode water electrolysis cycles with 0.5 M Na_2O_4 in the working compartment and 10 mM FcNCl together with 0.5 M Na_2SO_4 in the counter compartment. Ni_2P/Ni/NF and NF were utilized as the HER and OER electrodes, respectively, in the working chamber, and a carbon rod was used as the counter electrode in the counter chamber. Voltage bias between the working and counter electrodes was alternated at −1.6 V for HER and 1.8 V for OER periodically. No iR correction was applied.

combination of a PV cell (photovoltage >1.4 V) and FcNCl would be able to drive HER without any external bias. Hence, we connected a two-electrode H-type cell with the same configuration to a commercial PV cell (~1.6 V; Figure S12) to assess our hypothesis. Figure 4A shows the LSVs of HER collected on Ni_2P/Ni/NF in 0.5 M Na_2SO_4, where 10 mM FcNCl and 0.5 M Na_2SO_4 were loaded in the counter compartment with a carbon rod as the counter electrode. To reach a current density of -30 mA cm^{-2} for H_2 evolution, an external voltage bias of −1.58 V was required in the absence of natural sunlight irradiation. In contrast, when the solar cell was fully exposed to solar irradiation (intensity = 92 $\pm$ 5 mW cm^{-2}), the same current density could be achieved at zero external bias. Figure 4B displays the current evolution over time upon chopped solar irradiation, when the applied external bias was set at 0 V. When solar irradiation was not blocked, an immediate increase in cathodic current was observed, accompanied by vigorous H_2 bubble formation and release on the Ni_2P/NF working electrode. The periodic on and off catalytic HER current dependent on the sunlight exposure strongly supports the conclusion that the H_2 evolution detected was solely driven by sunlight irradiation. Control experiments under identical conditions but without FcNCl in the counter compartment demonstrated that FcNCl was crucial for this solar-driven decoupled H_2 evolution.

Decoupled Water Splitting and Organic Oxidation Using $Na_4[Fe(CN)_6]$

As demonstrated in the above discussion, the FcNCl electron reservoir is stable in the pH range of 5–9. To extend such electrolyzer designs to other applications, we also introduced $Na_4[Fe(CN)_6]$, which is stable in a wider pH range from neutral to alkaline (1.0 M NaOH) conditions, as a proton-independent electron reservoir. $Na_4[Fe(CN)_6]$ is a low-cost chemical with relatively high solubility (0.6 M) in water and multiple industrial applications.[40] The electrochemical results demonstrate that $Na_4[Fe(CN)_6]$ possesses a suitable redox feature located between the onset potentials of HER and OER catalyzed by Co-P and NF working electrodes, respectively (Figures S13–S16), with a large diffusion coefficient of 3.53×10^{-6} cm^2 s^{-1}

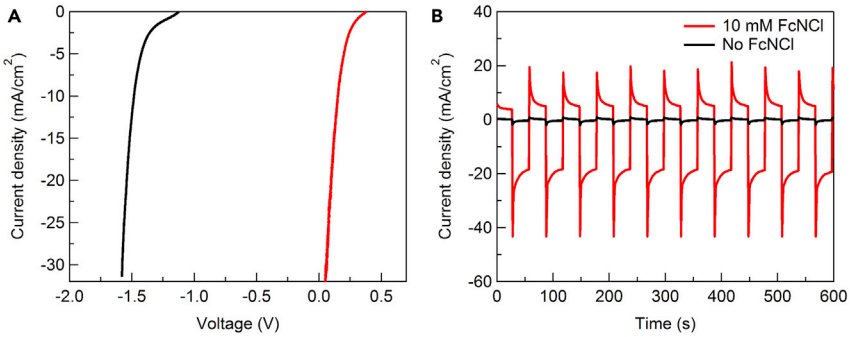

Figure 4. Electrocatalytic H_2 Evolution with the Assistance of a PV Cell under Natural Sunlight Irradiation

(A) Linear sweep voltammograms of HER on Ni_2P/Ni/NF in 0.5 M Na_2SO_4 with a carbon electrode in the counter chamber charged with 10 mM FcNCl and 0.5 M Na_2SO_4 with (red) and without (black) an external PV cell under sunlight irradiation (iR corrected).

(B) HER current density on Ni_2P/Ni/NF produced over time under chopped sunlight irradiation with no external voltage bias. Red curve, 10 mM FcNCl in the counter compartment; black curve, no FcNCl was added in the counter compartment. No iR correction was applied.

and an electron-transfer rate constant of 2.20×10^{-1} cm s^{-1}, as well as remarkable robustness in 0.5 M Na_2SO_4 and 0.5 M sodium phosphate buffer (NaPi, pH 7.0) electrolyte (Figure S17). The utilization of $Na_4[Fe(CN)_6]$ as an electron reservoir was shown to effectively split a large voltage input of one-step water splitting to two smaller voltage inputs for separate HER and OER processes with great cycling stability and a Faradic efficiency of 100% under neutral conditions (Figures S18–S21). The energy efficiency was calculated to be 64.6%, comparable with that of other decoupled water-splitting systems in acidic or alkaline electrolytes (Table S1). In addition, PV cells with small photovoltages (1.1 or 1.6 V; Figure S22) were also able to drive decoupled water splitting under natural sunlight irradiation when $Na_4[Fe(CN)_6]$ was used as the electron reservoir (Figures S23 and S24).[7,23] Further optimization of the PV-electrolyzer design in terms of the sizes of PV panels and electrodes, concentrations of the electron reservoir, and power densities of PV and electrolyzer will be pursued for achieving high solar-to-H_2 efficiency.

Given that O_2 generated from water splitting is not a product of high value, we reasoned that it would be more economically attractive if our electron reservoir could be further utilized to promote HER and other organic upgrading reactions, such as electrochemical reforming of biomass-derived intermediates.[22,41] For instance, HMF is an intermediate platform chemical produced from biomass materials, which can be transformed to many value-added products.[42] Previous studies have demonstrated that HMF can be readily oxidized to more valuable FDCA by Ni-based electrocatalysts under alkaline conditions.[43,44] The electrochemical experiments of $Na_4[Fe(CN)_6]$ conducted in 1.0 M NaOH proved that its redox feature (1.3 V versus RHE) was still positioned between the HER and OER onset potentials and less positive than the HMF oxidation on NF under alkaline conditions (Figure S25) with a diffusion coefficient of 4.70×10^{-6} cm^2 s^{-1} and an electron-transfer rate constant of 8.45×10^{-2} cm s^{-1} (Figure S26), which were comparable with the reported values.[45] The negligible degradation during 1,000 redox cycles of $Na_4[Fe(CN)_6]$ in 1.0 M NaOH further demonstrated its excellent stability.

Therefore, similar to decoupled water splitting, a two-compartment electrochemical cell with a cation exchange membrane was utilized for HER and HMF oxidation in 1.0 M NaOH (Scheme 1C). Figure 5A compares the LSV curves of a Co-P working electrode

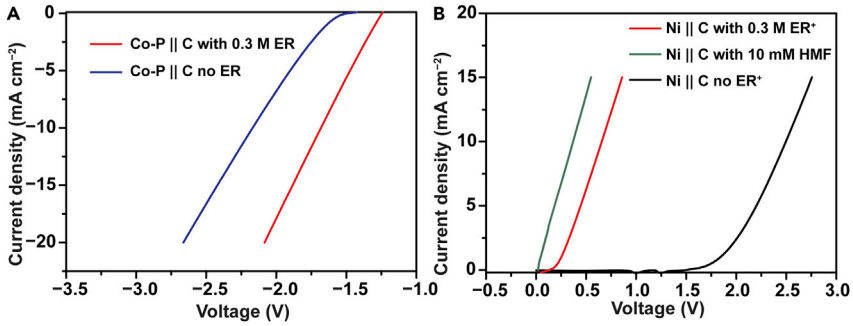

Figure 5. Electrochemical Investigation of Decoupled HER, OER, and HMF Oxidation with the Assistance of $Na_4[Fe(CN)_6]$ as an Electron Reservoir

(A) Linear sweep voltammograms of the two-electrode H-cell systems consisting of a Co-P working electrode and a carbon counter electrode with (red) or without (blue) 0.3 M $Na_4[Fe(CN)_6]$ (ER) in the counter compartment.

(B) Linear sweep voltammograms of the two-electrode H-cell systems consisting of a Ni foam working electrode and a carbon counter electrode under different conditions: neither $Na_3[Fe(CN)_6]$ (ER^+) nor HMF in both compartments (black); 0.3 M ER^+ in the counter compartment (red); or 10 mM HMF in the working compartment and 0.3 M ER^+ in the counter compartment (green). The common electrolyte for all of the above experiments was 1.0 M NaOH. No results were iR corrected.

for HER with and without 0.3 M $Na_4[Fe(CN)_6]$ in the counter compartment. The addition of the electron reservoir substantially shifted the LSV curve of HER toward the positive direction. After the 0.3 M $Na_4[Fe(CN)_6]$ in the counter chamber had been oxidized in a chronocoulometry experiment, an LSV curve was collected on the NF working electrode for OER (Figure 5B), which delivered 10 mA cm^{-2} at a voltage bias of 0.66 V. However, upon the addition of 10 mM HMF in the working chamber, a less positive onset potential was observed for HMF oxidation, achieving 10 mA cm^{-2} at a voltage bias of only 0.37 V. Chronocoulometry electrolysis for HMF oxidation was conducted at a voltage bias of 0.2 V. After passing 87 C charge, the conversion of HMF reached 100%, resulting in an FDCA yield of 83% (Figure S27) without the need for noble-metal catalysts, which were widely used in previous reports.[46–48] It is anticipated that HER coupled with electron reservoir oxidation can be driven by PV under diurnal sunlight irradiation, and electrocatalytic HMF oxidation is carried out at a small voltage (e.g., 0.2 V) coupled with electron reservoir regeneration at night with this novel electrolyzer design.[49] Exploration of new electron reservoirs with higher solubility is preferred for increasing the capacity of the electron reservoir solutions.

Conclusions

In summary, we have reported that a ferrocene-derived complex FcNCl can act as a robust and low-cost electron reservoir for decoupled water electrolysis under near-neutral conditions. Such a decoupling strategy enables H_2 and O_2 to be produced at different times and the production rate of one gas to be independent of the other, allowing fast H_2 production at elevated pressure without the concern of H_2/O_2 mixing. The reversible redox couple, high solubility, and great robustness of FcNCl in water make it feasible to conduct decoupled water electrolysis in near-neutral water with earth-abundant electrocatalysts. Thanks to the substantially reduced voltage requirement for HER based on this decoupling approach, we further demonstrated that a PV cell with a small photovoltage (~1.6 V) was able to drive efficient H_2 evolution (~20 mA cm^{-2}) under natural sunlight irradiation without any external bias. Furthermore, we also introduced another electron reservoir, $Na_4[Fe(CN)_6]$, which is stable in a wider pH range from neutral to alkaline conditions. The low cost, high solubility, remarkable robustness, and excellent redox properties of

$Na_4[Fe(CN)_6]$ render it an ideal electron reservoir not only for decoupled water splitting in neutral electrolyte but also for HER integrated with organic upgrading under alkaline conditions. This work offers attractive economic and safety advantages for sustainable H_2 production from water and also allows great flexibility in electrolyzer design for water electrolysis and electrocatalytic organic upgrading. This work will inspire researchers to explore novel electron reservoirs with lower cost, higher solubility, and better-positioned redox potential for decoupled water electrolysis and other promising electrocatalytic applications such as biocatalytic reactions, biomass valorization, and seawater electrolysis.

EXPERIMENTAL PROCEDURES

Full experimental procedures are provided in the Supplemental Information.

SUPPLEMENTAL INFORMATION

Supplemental Information includes Supplemental Experimental Procedures, 27 figures, and 1 table and can be found with this article online at https://doi.org/10.1016/j.chempr.2017.12.019.

ACKNOWLEDGMENTS

We acknowledge the support of the National Science Foundation (CHE-1653978) and the Microscopy Core Facility at Utah State University. N.J. thanks the School of Graduate Studies Dissertation Fellowship of Utah State University.

AUTHOR CONTRIBUTIONS

Y.S. designed and supervised the project, directed the research, analyzed and interpreted the data, and wrote the manuscript. W.L. and N.J. designed the methodology and conducted the experiments, prepared samples, analyzed and interpreted the data, and wrote the manuscript. W.L. and N.J. contributed equally to this work. B.H. and T.L.L. provided FcNCl and SELEMIONTM AMV membranes. X.L. contributed to SEM and elemental mapping measurements and assisted with sample preparation. F.S. assisted with XRD and some electrochemical measurements. G.H. assisted with HPLC and GC experiments. T.J.J. and T.B.H. assisted with solar-driven water-splitting experiments. All of the authors discussed the results and reviewed the manuscript.

DECLARATION OF INTERESTS

The authors declare no competing interests.

Received: August 2, 2017
Revised: October 20, 2017
Accepted: December 19, 2017
Published: February 1, 2018

REFERENCES AND NOTES

1. Lewis, N.S., and Nocera, D.G. (2006). Powering the planet: chemical challenges in solar energy utilization. Proc. Natl. Acad. Sci. USA *103*, 15729–15735.

2. Gray, H.B. (2009). Powering the planet with solar fuel. Nat. Chem. *1*, 7.

3. Cook, T.R., Dogutan, D.K., Reece, S.Y., Surendranath, Y., Teets, T.S., and Nocera, D.G. (2010). Solar energy supply and storage for the legacy and nonlegacy worlds. Chem. Rev. *110*, 6474–6502.

4. Walter, M.G., Warren, E.L., McKone, J.R., Boettcher, S.W., Mi, Q., Santori, E.A., and Lewis, N.S. (2010). Solar water splitting cells. Chem. Rev. *110*, 6446–6473.

5. Ursua, A., Gandia, L.M., and Sanchis, P. (2012). Hydrogen production from water electrolysis: current status and future trends. Proc. IEEE *100*, 410–426.

6. Carmo, M., Fritz, D.L., Mergel, J., and Stolten, D. (2013). A comprehensive review on PEM water electrolysis. Int. J. Hydrogen Energy *38*, 4901–4934.

7. Jia, J., Seitz, L.C., Benck, J.D., Huo, Y., Chen, Y., Ng, J.W.D., Bilir, T., Harris, J.S., and Jaramillo, T.F. (2016). Solar water splitting by

photovoltaic-electrolysis with a solar-to-hydrogen efficiency over 30%. Nat. Commun. *7*, 13237.

8. Symes, M.D., and Cronin, L. (2013). Decoupling hydrogen and oxygen evolution during electrolytic water splitting using an electron-coupled-proton buffer. Nat. Chem. *5*, 403–409.

9. Chen, L., Dong, X., Wang, Y., and Xia, Y. (2016). Separating hydrogen and oxygen evolution in alkaline water electrolysis using nickel hydroxide. Nat. Commun. *7*, 11741.

10. Jin, J., Walczak, K., Singh, M.R., Karp, C., Lewis, N.S., and Xiang, C. (2014). An experimental and modeling/simulation-based evaluation of the efficiency and operational performance characteristics of an integrated, membrane-free, neutral pH solar-driven water-splitting system. Energy Environ. Sci. *7*, 3371–3380.

11. Berger, A., Segalman, R.A., and Newman, J. (2014). Material requirements for membrane separators in a water-splitting photoelectrochemical cell. Energy Environ. Sci. *7*, 1468–1476.

12. Bloor, L.G., Solarska, R., Bienkowski, K., Kulesza, P.J., Augustynski, J., Symes, M.D., and Cronin, L. (2016). Solar-driven water oxidation and decoupled hydrogen production mediated by an electron-coupled-proton buffer. J. Am. Chem. Soc. *138*, 6707–6710.

13. Barbir, F. (2005). PEM electrolysis for production of hydrogen from renewable energy sources. Sol. Energy *78*, 661–669.

14. Ghassemzadeh, L., Kreuer, K.-D., Maier, J., and Müller, K. (2010). Chemical degradation of Nafion membranes under mimic fuel cell conditions as investigated by solid-state NMR spectroscopy. J. Phys. Chem. C *114*, 14635–14645.

15. Prabhakaran, V., Arges, C.G., and Ramani, V. (2012). Investigation of polymer electrolyte membrane chemical degradation and degradation mitigation using in situ fluorescence spectroscopy. Proc. Natl. Acad. Sci. USA *109*, 1029–1034.

16. Rausch, B., Symes, M.D., and Cronin, L. (2013). A bio-inspired, small molecule electron-coupled-proton buffer for decoupling the half-reactions of electrolytic water splitting. J. Am. Chem. Soc. *135*, 13656–13659.

17. Amstutz, V., Toghill, K.E., Powlesland, F., Vrubel, H., Comninellis, C., Hu, X., and Girault, H.H. (2014). Renewable hydrogen generation from a dual-circuit redox flow battery. Energy Environ. Sci. *7*, 2350–2358.

18. Peljo, P., Vrubel, H., Amstutz, V., Pandard, J., Morgado, J., Santasalo-Aarnio, A., Lloyd, D., Gumy, F., Dennison, C.R., Toghill, K.E., and Girault, H.H. (2016). All-vanadium dual circuit redox flow battery for renewable hydrogen generation and desulfurization. Green Chem. *18*, 1785–1797.

19. Moreno-Hernandez, I.A., MacFarland, C.A., Read, C.G., Papadantonakis, K.M., Brunschwig, B.S., and Lewis, N.S. (2017). Crystalline nickel manganese antimonate as a stable water-oxidation catalyst in aqueous 1.0 M H_2SO_4. Energy Environ. Sci. *10*, 2103–2108.

20. Xiang, C., Papadantonakis, K.M., and Lewis, N.S. (2016). Principles and implementations of electrolysis systems for water splitting. Mater. Horiz. *3*, 169–173.

21. Landman, A., Dotan, H., Shter, G.E., Wullenkord, M., Houaijia, A., Maljusch, A., Grader, G.S., and Rothschild, A. (2017). Photoelectrochemical water splitting in separate oxygen and hydrogen cells. Nat. Mater. *16*, 646–651.

22. Chen, Y.X., Lavacchi, A., Miller, H.A., Bevilacqua, M., Filippi, J., Innocenti, M., Marchionni, A., Oberhauser, W., Wang, L., and Vizza, F. (2014). Nanotechnology makes biomass electrolysis more energy efficient than water electrolysis. Nat. Commun. *5*, 4036.

23. Luo, J., Im, J.H., Mayer, M.T., Schreier, M., Nazeeruddin, M.K., Park, N.-G., Tilley, S.D., Fan, H.J., and Grätzel, M. (2014). Water photolysis at 12.3% efficiency via perovskite photovoltaics and Earth-abundant catalysts. Science *345*, 1593–1596.

24. Sakimoto, K.K., Wong, A.B., and Yang, P. (2016). Self-photosensitization of nonphotosynthetic bacteria for solar-to-chemical production. Science *351*, 74–77.

25. Liu, C., Colón, B.C., Ziesack, M., Silver, P.A., and Nocera, D.G. (2016). Water splitting–biosynthetic system with CO_2 reduction efficiencies exceeding photosynthesis. Science *352*, 1210–1213.

26. Liu, C., Gallagher, J.J., Sakimoto, K.K., Nichols, E.M., Chang, C.J., Chang, M.C.Y., and Yang, P. (2015). Nanowire–bacteria hybrids for unassisted solar carbon dioxide fixation to value-added chemicals. Nano Lett. *15*, 3634–3639.

27. Nichols, E.M., Gallagher, J.J., Liu, C., Su, Y., Resasco, J., Yu, Y., Sun, Y., Yang, P., Chang, M.C.Y., and Chang, C.J. (2015). Hybrid bioinorganic approach to solar-to-chemical conversion. Proc. Natl. Acad. Sci. USA *112*, 11461–11466.

28. Hu, B., DeBruler, C., Rhodes, Z., and Liu, T.L. (2017). Long-cycling aqueous organic redox flow battery (AORFB) toward sustainable and safe energy storage. J. Am. Chem. Soc. *139*, 1207–1214.

29. Li, W., Gao, X., Xiong, D., Xia, F., Liu, J., Song, W.-G., Xu, J., Thalluri, S.M., Cerqueira, M.F., Fu, X., et al. (2017). Vapor-solid synthesis of monolithic single-crystalline CoP nanowire electrodes for efficient and robust water electrolysis. Chem. Sci. *8*, 2952–2958.

30. Burke, M.S., Kast, M.G., Trotochaud, L., Smith, A.M., and Boettcher, S.W. (2015). Cobalt–iron (oxy)hydroxide oxygen evolution electrocatalysts: the role of structure and composition on activity, stability, and mechanism. J. Am. Chem. Soc. *137*, 3638–3648.

31. Li, W., Gao, X., Xiong, D., Wei, F., Song, W.-G., Xu, J., and Liu, L. (2017). Hydrothermal synthesis of monolithic Co_3Se_4 nanowire electrodes for oxygen evolution and overall water splitting with high efficiency and extraordinary catalytic stability. Adv. Energy Mater. *7*, 1602579.

32. Burke, M.S., Zou, S., Enman, L.J., Kellon, J.E., Gabor, C.A., Pledger, E., and Boettcher, S.W. (2015). Revised oxygen evolution reaction activity trends for first-row transition-metal (oxy)hydroxides in alkaline media. J. Phys. Chem. Lett. *6*, 3737–3742.

33. Li, W., Gao, X., Wang, X., Xiong, D., Huang, P.-P., Song, W.-G., Bao, X., and Liu, L. (2016). From water reduction to oxidation: janus Co-Ni-P nanowires as high-efficiency and ultrastable electrocatalysts for over 3000 h water splitting. J. Power Sources *330*, 156–166.

34. You, B., Liu, X., Hu, G., Gul, S., Yano, J., Jiang, D.E., and Sun, Y. (2017). Universal surface engineering of transition metals for superior electrocatalytic hydrogen evolution in neutral water. J. Am. Chem. Soc. *139*, 12283–12290.

35. Li, W., Xiong, D., Gao, X., Song, W.-G., Xia, F., and Liu, L. (2017). Self-supported Co-Ni-P ternary nanowire electrodes for highly efficient and stable electrocatalytic hydrogen evolution in acidic solution. Catal. Today *287*, 122–129.

36. Li, W., Wang, X., Xiong, D., and Liu, L. (2016). Efficient and durable electrochemical hydrogen evolution using cocoon-like MoS_2 with preferentially exposed edges. Int. J. Hydrogen Energy *41*, 9344–9354.

37. Rausch, B., Symes, M.D., Chisholm, G., and Cronin, L. (2014). Decoupled catalytic hydrogen evolution from a molecular metal oxide redox mediator in water splitting. Science *345*, 1326–1330.

38. Bockris, J., Conway, B., Yeager, E., and White, R. (1981). Comprehensive Treatise of Electrochemistry: Electrochemical Processing (Plenum Press).

39. Qi, Z. (2013). Proton Exchange Membrane Fuel Cells (CRC Press).

40. Grieken, R., Aguado, J., López-Muñoz, M.-J., and Marugán, J. (2005). Photocatalytic degradation of iron-cyanocomplexes by TiO_2 based catalysts. Appl. Catal. B Environ. *55*, 201–211.

41. Cha, H.G., and Choi, K.-S. (2015). Combined biomass valorization and hydrogen production in a photoelectrochemical cell. Nat. Chem. *7*, 328–333.

42. Zhang, Z., and Deng, K. (2015). Recent advances in the catalytic synthesis of 2,5-furandicarboxylic acid and its derivatives. ACS Catal. *5*, 6529–6544.

43. You, B., Liu, X., Jiang, N., and Sun, Y. (2016). A general strategy for decoupled hydrogen production from water splitting by integrating oxidative biomass valorization. J. Am. Chem. Soc. *138*, 13639–13646.

44. You, B., Jiang, N., Liu, X., and Sun, Y. (2016). Simultaneous H_2 generation and biomass upgrading in water by an efficient noble-metal-free bifunctional electrocatalyst. Angew. Chem. Int. Ed. *55*, 9913–9917.

45. Gong, K., Xu, F., Grunewald, J.B., Ma, X., Zhao, Y., Gu, S., and Yan, Y. (2016). All-soluble all-iron aqueous redox-flow battery. ACS Energy Lett. *1*, 89–93.

46. Davis, S.E., Houk, L.R., Tamargo, E.C., Datye, A.K., and Davis, R.J. (2011). Oxidation of 5-hydroxymethylfurfural over supported Pt, Pd and Au catalysts. Catal. Today *160*, 55–60.

47. Gorbanev, Y.Y., Klitgaard, S.K., Woodley, J.M., Christensen, C.H., and Riisager, A. (2009). Gold-catalyzed aerobic oxidation of 5-hydroxymethylfurfural in water at ambient temperature. ChemSusChem *2*, 672–675.

48. Chen, C., Yu, Y., Li, W., Cao, C., Li, P., Dou, Z., and Song, W. (2011). Mesoporous $Ce_{1-x}Zr_xO_2$ solid solution nanofibers as high efficiency catalysts for the catalytic combustion of VOCs. J. Mater. Chem. *21*, 12836–12841.

49. Mallouk, T.E. (2013). Water electrolysis: divide and conquer. Nat. Chem. *5*, 362–363.